Electronic Supplementary Material (ESI) for New Journal of Chemistry.

A bis(thiosemicarbazonato)-copper complex, a new catalyst for electro- and photo-reduction of CO_2 to methanol

Wen-Xing Jiang, Wei-Xia Liu, Chun-Li Wang, Shu-Zhong Zhan*, Song-Ping Wu*

College of Chemistry & Chemical Engineering, South China University of Technology, Guangzhou 510640, China

Supplementary Materials

Table of context

1	**Physical measurements**
2	**Crystal structure determination**
3	**Fig. S1.** XRD spectra of Au-CdS NCs and the related samples.
4	**Fig. S2.** ^{1}H NMR (600 MHz, DMSO-d6) spectra of H_2ATSM.
5	**Fig. S3**. ESI-MS of the copper complex, Cu-ATSM in methanol.
6	**Fig. S4.** (a) Scan rate dependence of precatalytic waves for 1.50 mM Cu-ATSM (0.1 M [n-Bu_4N]ClO_4) in a DMF solution under an atmosphere of N_2. Scan rates vary from 50 to 300 mV·s^{-1}. Fc internal standard (*). (b) Scan rate dependence of precatalytic waves for the Cu$^{II/I}$ couple of 1.50 mM Cu-ATSM. (c) Scan rate dependence of precatalytic waves for the Cu$^{III/II}$ couple of 1.50 mM Cu-ATSM.
7	**Fig. S5.** CVs of a CO_2-saturated DMF solution with the copper complex (1.50 mM) in the varying amount of methanol. Conditions: glassy carbon working electrode (1.0 mm diameter), Pt counter electrode, Ag/$AgNO_3$ reference electrode, scan rate 100 mV·s^{-1}. Fc internal standard (*).

16	**Fig. S14.** The selectivity for CO_2 reduction products from the photolysis of the CO_2-saturated $KHCO_3$ (0.10 M) solution (pH 5.0) containing 0.10 mg·mL^{-1} CdS NRs, 0.10 M ascorbic acid and 0.01 mM Cu-ATSM.
17	**Fig. S15.** (a) GC-MS spectrum of $^{13}CO_2$ reduction product mediated by CuATSM. (b) The standard spectrum of $^{13}CH_3OH$.
18	**Fig. S16.** pH values change of the catalytic system containing CO_2 (1 atm), 0.10 M ascorbic acid, 0.10 mg.mL^{-1} Au-CdS NCs and 0.01 mM Cu-ATSM during photolysis.
19	**Fig. S17.** XPS spectra of the photocatalyst samples. The lower line is for the mixture of Au-CdS NCs and Cu-ATSM. The upper line is the photocatalyst after the CO_2 reduction reaction, which was centrifuged and washed by water after 40 hours of irradiation. (a) High resolution spectra of Cu 2p peaks at 932.18 eV and 952.20 eV. (b) High resolution spectra of S 2p peaks at 162.33 eV and 163.52 eV. (c) High resolution spectra of N 1s and Cd 3d peaks at 398.49 eV, 399.62 eV, 402.47 eV, 405.29 eV and 412.05 eV. (d) High resolution spectra of Au 4f peaks at 84.21 eV and 87.87 eV.
20	**Fig. S18.** (a) UV-vis diffuse reflectance spectra of the prepared Au-CdS NCs (black line), Cu-ATSM (blue line) and the mixture of Cu-ATSM and Au-CdS NCs (red line). (b) The estimated band gap spectra obtained from (a).
21	**Fig. S19**. XPS valence band spectrum of Au-CdS NCs.
22	**Fig. S20.** Electrochemical impedance spectroscopy Nyquist plots of Au-CdS NCs and Au-CdS NCs/Cu-ATSM with FTO electrode (1 cm^2) in 0.010 M $K_3Fe(CN)_6$/ $K_4Fe(CN)_6$ electrolyte in the dark.
23	**Table S1** Crystallographic data for the copper complex, Cu-ATSM
24	**Table S2** Selected bond lengths (Å) for the copper complex, Cu-ATSM

Physical measurements

NMR analysis was conducted by using a Bruker AV-500 instrument. UV-Vis spectra were measured on a Hitachi U-3010. The electrochemical impedance spectra (EIS) measurements were performed in the presence of a 0.010 M $K_3[Fe(CN)_6]/K_4[Fe(CN)_6]$ (1:1) mixture as a redox probe in 0.10 M KCl solution. Measurements and analysis for the chemical compositions and valence states of the photocatalysts were carried out by ESCALAB 250 Xi X-photoelectron spectroscopy (XPS) with monochromatic Al Kα (1486.6 eV) X-ray sources. Measurements and analysis for the crystalline diffraction patterns of Au-CdS NCs and the related components were carried out by using Bruker D8 Advance powder X-ray diffraction. Transmission Electron Microscopy (TEM) images were afforded by using a JEM-2010 electron microscope. Scanning electron microscopy (SEM) images were obtained on a Merlin emission gun SEM instrument.

The electrochemical measurements were performed on a conventional three-electrode system at CHI 660E electrochemical workstation (Chenhua, Shanghai, China), in which platinum electrode as counter electrode and saturated calomel electrode (SCE) as reference electrode for constant-potential electrolysis (CPE) and $Ag/AgNO_3$ electrode as reference electrode for Cyclic voltammograms (CVs). The working electrode for CVs is glassy carbon electrode ($\Phi = 1$ mm), and the working electrode for CPE was fabricated through loading sample suspension onto the FTO electrode. Firstly, 10 mg Cu-ATSM electrocatalyst was dispersed in 5 mL water and sonicated for 15 min to form a 2 mg·mL^{-1} homogeneous suspension. Then, 50 μL of the well-dispersed catalyst suspension was loaded onto the FTO electrode, which gives the loading of electrocatalyst was about 0.1 mg. After drying under an infrared lamp, 20 μL of 0.445 wt% Nafion solution (1 mL 5 wt% Nafion solution + 5 mL H_2O + 5 mL absolute ethanol) was dropped onto the surface of the catalyst layer to form a thin protective film and then dried under an infrared lamp. CO_2 reduction experiments were carried out in 30 mL CO_2-saturated 0.1 M $KHCO_3$ (pH 6.7) aqueous solution.

For the photocatalytic system, each sample was prepared in a flask of buffer solution with CO_2 (1 atm), ascorbic acid, Au-CdS NCs, and the copper complex. Then, the flask was sealed with a septum. At room temperature, blue light (469 nm) was used to irradiate each sample. After electrocatalysis or photocatalysis, the CO_2 reduction products in gas phase were detected by the gas chromatograph (GC). GC experiments were carried out with an Agilent Technologies 7890A gas chromatography instrument. The CO_2 reduction products in liquid phase from electrolysis or photolysis were detected by NMR spectroscopy.

Crystal structure determination

Crystallographic data collections for the copper complex was performed on a Bruker Smart Apex II DUO area detector. The SADABS program was employed to correct absorption effects in the copper complex, [42] and the direct methods was used to determine the crystal structure. The SHELXTL-97 computer program was used to perform the calculations and structural analysis, [43] giving the results listed in Table S1. The selected bond lengths of the copper complex were listed in Table S2.

42 G. M. Sheldrick, SADABS, Program for Empirical Absorption Correction of Area Detector Data, University of Götingen, Götingen, Germany; 1996.

43 G. M. Sheldrick, *Acta Crystallographica Section A.*, 2008, **A64**, 112-122.

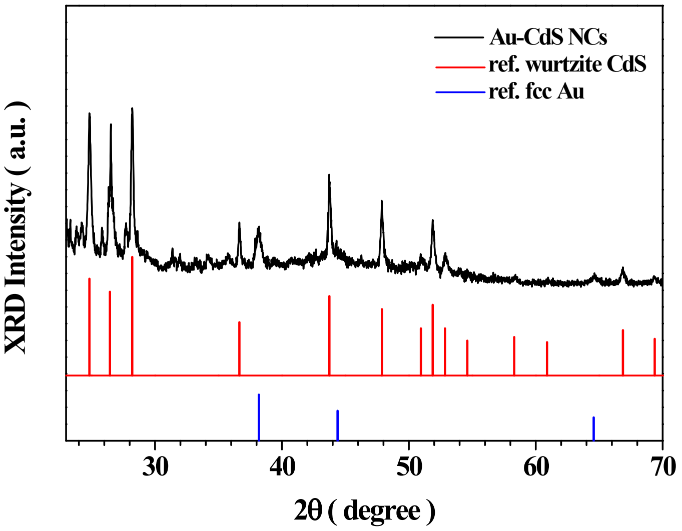

Fig. S1. XRD spectra of Au-CdS NCs and the related samples.

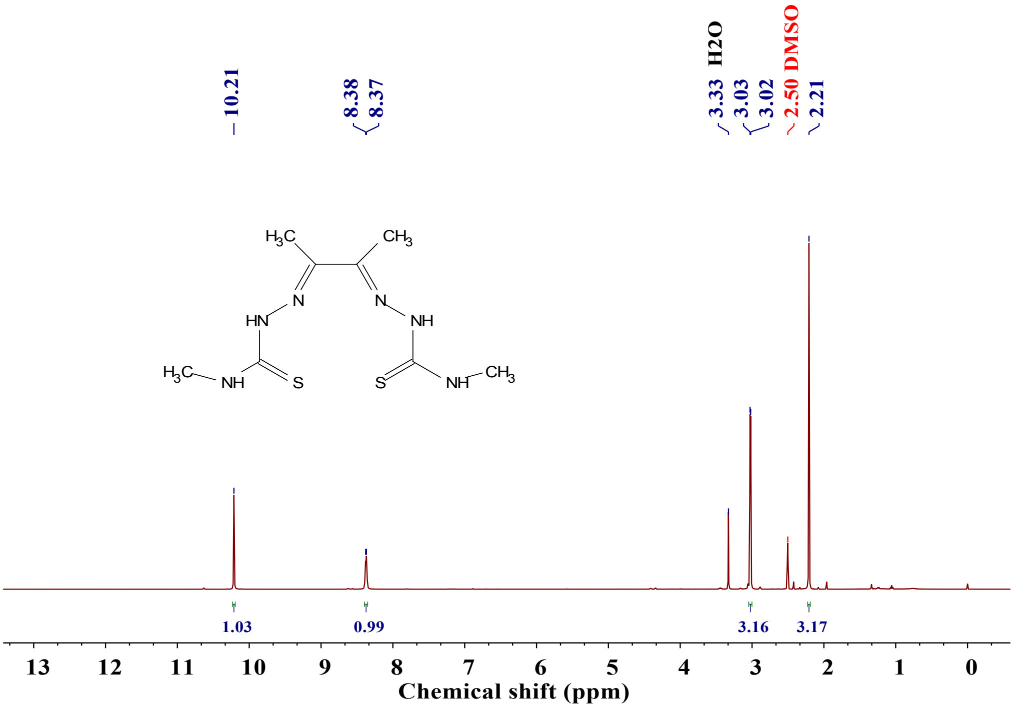

Fig. S2. ^{1}H NMR (600 MHz, DMSO-d6) spectra of H_2ATSM: δ/ppm 10.21 (2H, s, 2 × C=NNH), 8.37 and 8.38 (2H, two overlapping singlets, 2 × C(=S)NHCH3), 3.03 and 3.02 (6H, two overlapping singlets, 2 × C(=S)NHCH3), 2.21 (6H, s, CH_3CCCH_3).

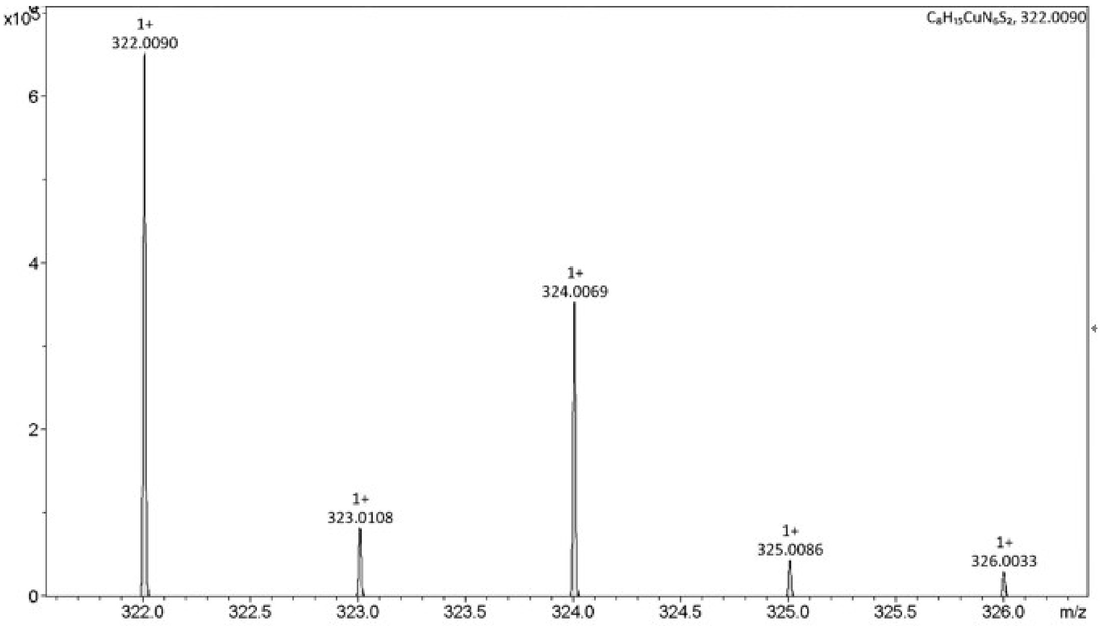

Fig. S3. ESI-MS of the copper complex, Cu-ATSM in methanol.

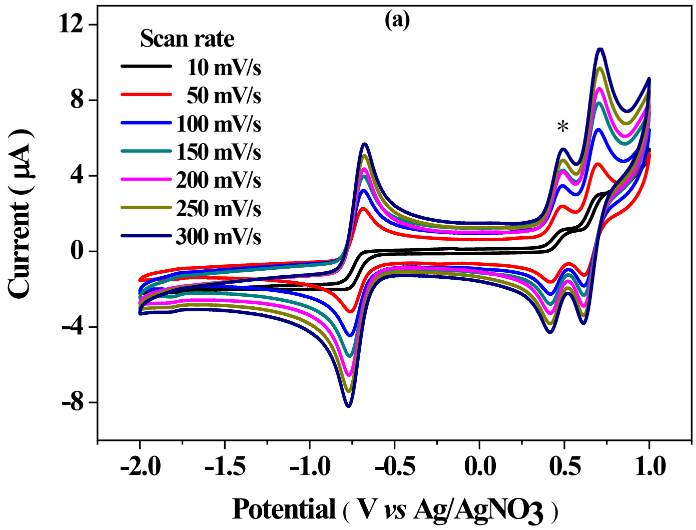

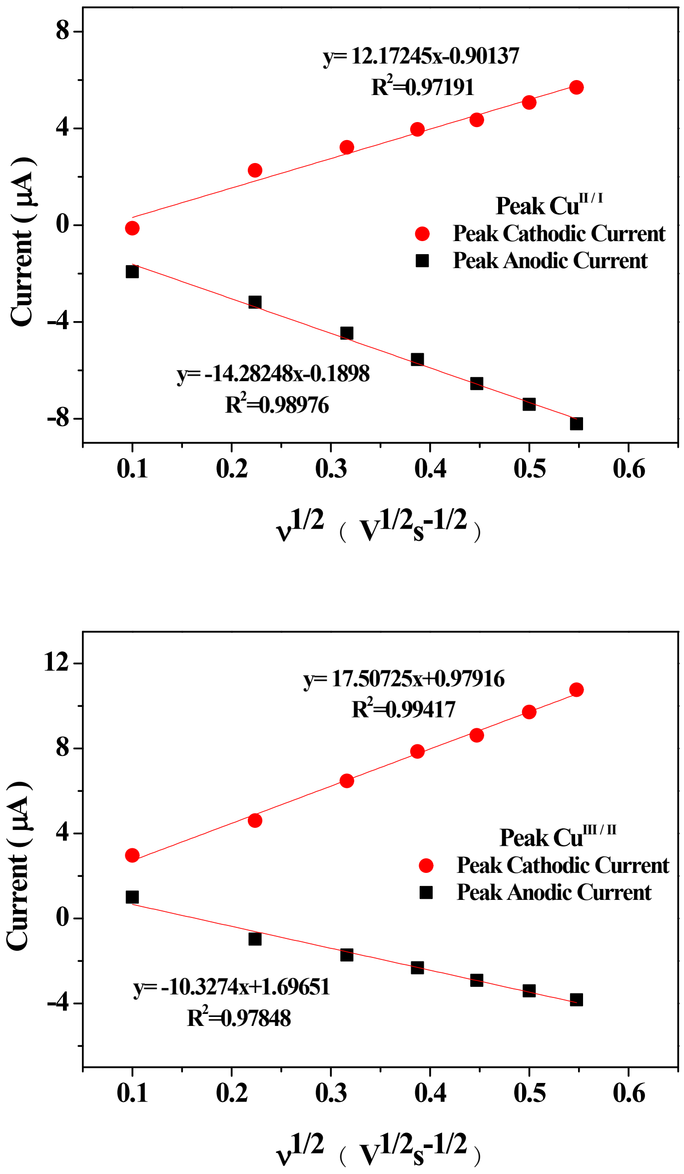

Fig. S4. (a) Scan rate dependence of precatalytic waves for 1.50 mM Cu-ATSM (0.1 M [n-Bu_4N]ClO_4) in a DMF solution under an atmosphere of N_2. Scan rates vary from 50 to 300 mV·s^{-1}. Fc internal standard (*). (b) Scan rate dependence of precatalytic waves for the $Cu^{II/I}$ couple of 1.50 mM Cu-ATSM. (c) Scan rate dependence of precatalytic waves for the $Cu^{III/II}$ couple of 1.50 mM Cu-ATSM.

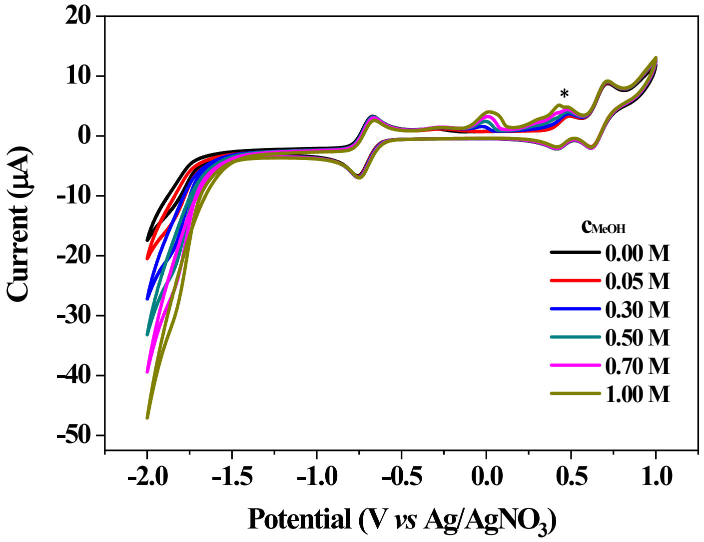

Fig. S5. CVs of a CO_2-saturated DMF solution with the copper complex (1.50 mM) in the varying amount of methanol. Conditions: glassy carbon working electrode (1.0 mm diameter), Pt counter electrode, $Ag/AgNO_3$ reference electrode, scan rate 100 $mV \cdot s^{-1}$. Fc internal standard (*).

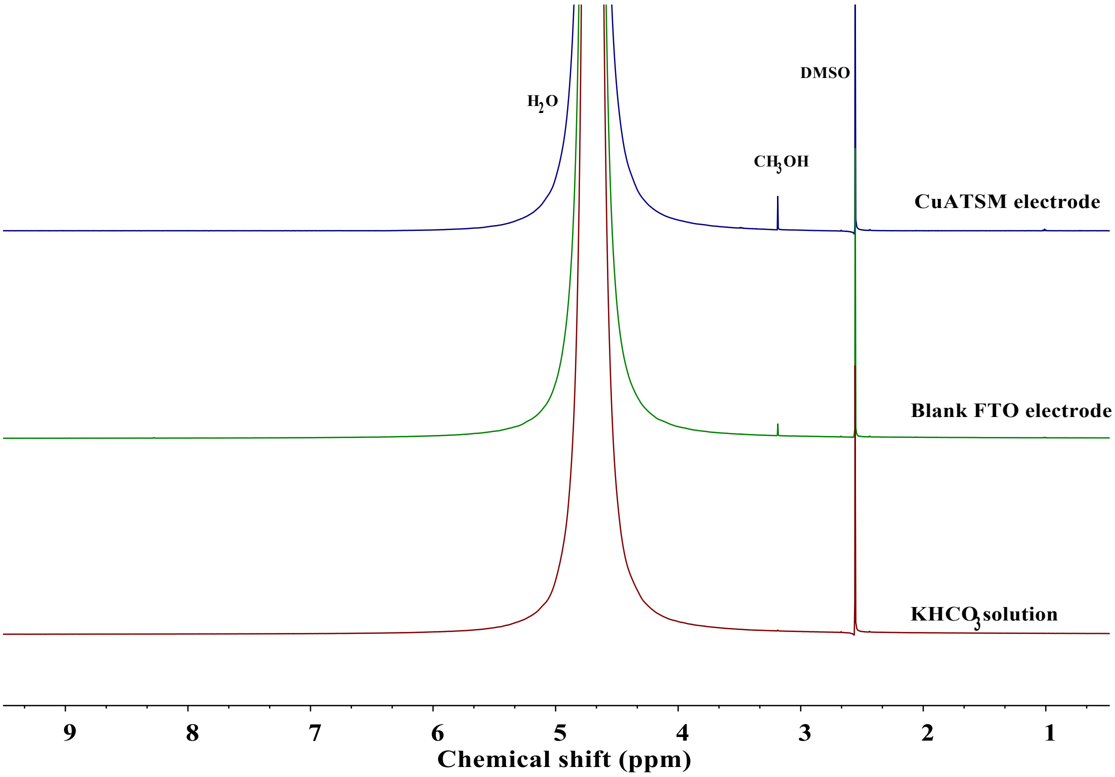

Fig. S6. ^1H NMR spectra of a CO_2-saturated $KHCO_3$ solution (0.10 M) before and after electrolysis for 2 h with different electrodes under -1.05 V versus Ag/AgCl.

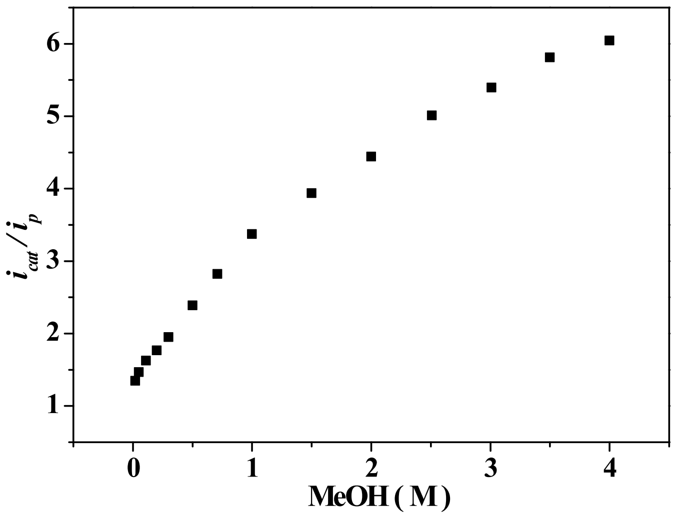

Fig. S7. Dependence of $i_{\mathrm{cat}}/i_{\mathrm{p}}$ on concentration of methanol based the couple of $\mathrm{Cu}^{\mathrm{I/0}}$. Conditions: CO_2-saturated DMF solution with 0.25 mM Cu-ATSM in 0.10 M [n-Bu_4N]ClO_4, scan rate 100 mV·s^{-1}.

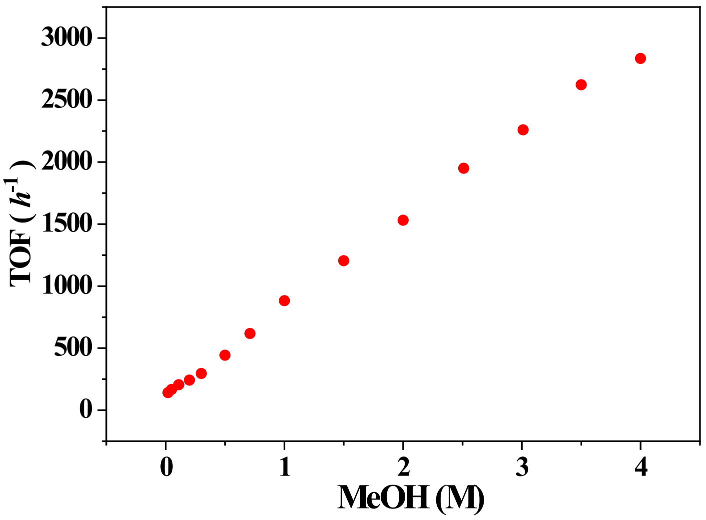

Fig. S8. TOFs for methanol production. Conditions: CO_2-saturated DMF solution with 1.50 mM Cu-ATSM in 0.10 M [n-Bu_4N], scan rate 100 mV·s^{-1}.

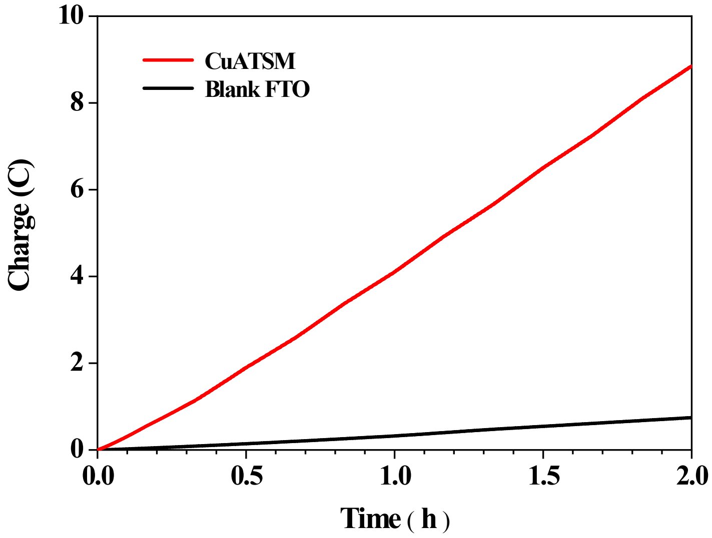

Fig. S9. Charge build-up versus time from electrolysis of a CO_2-saturated solution with 0.25 mM Cu-ATSM (0.10 M $KHCO_3$) under -1.05 V versus Ag/AgCl.

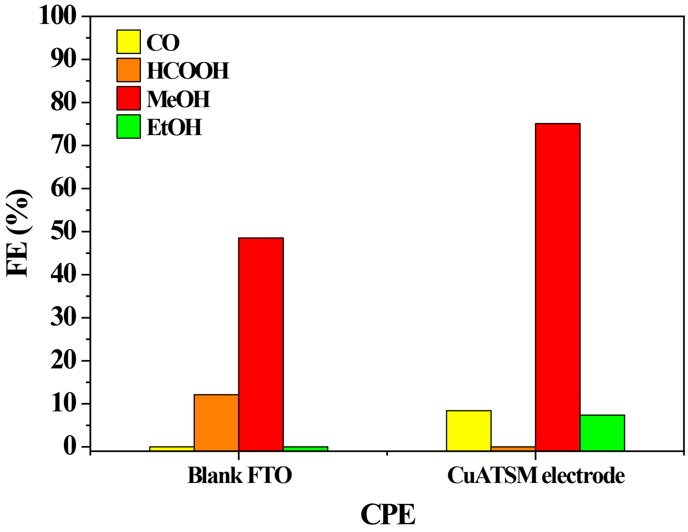

Fig. S10. Products obtained from the electrocatalytic reaction of a CO_2-saturated solution used 2 h containing 0.10 M $KHCO_3$ and 0.25 mM Cu-ATSM with different electrodes under -1.05 V versus Ag/AgCl.

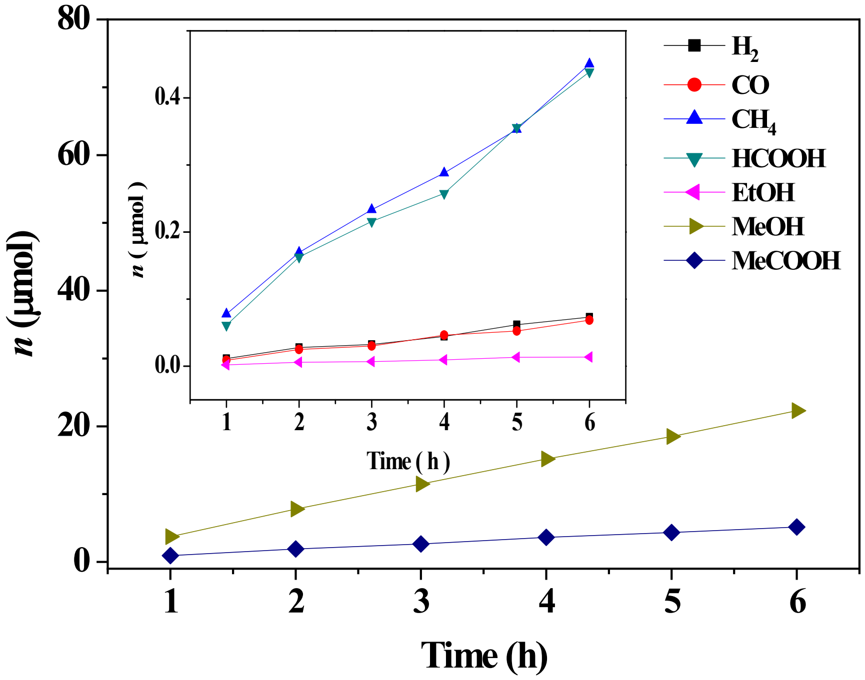

Fig. S11. Photocatalytic products from CO_2 reduction mediated by Cu-ATSM under visible light (λ = 469 nm). The reaction system contains 0.10 mg·mL^{-1} Au-CdS NCs, 0.010 mM Cu-ATSM and 0.10 M ascorbic acid (pH 5.0).

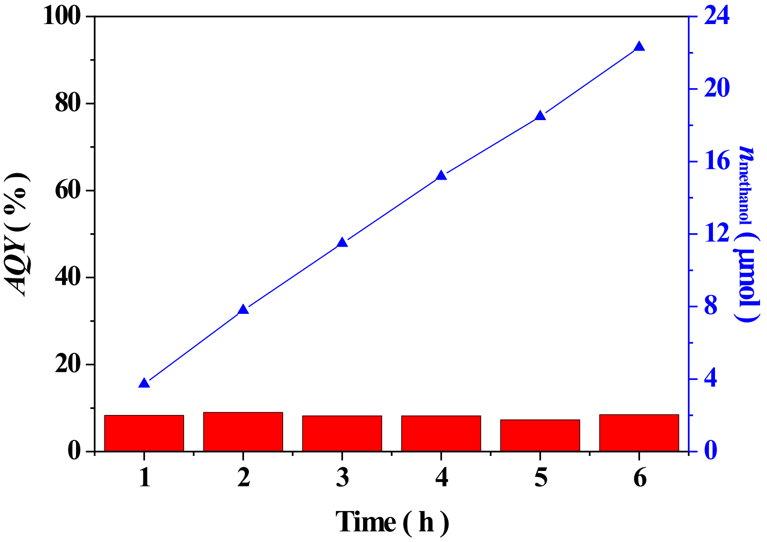

Fig. S12. Photocatalytic methanol production from CO_2 reduction mediated by Cu-ATSM under visible light (λ = 469 nm) and an apparent quantum yield (AQY) of Cu-ATSM under monochromatic light (λ= 469 nm). The reaction system contains 0.10 mg·mL^{-1} Au-CdS NCs, 0.010 mM Cu-ATSM and 0.10 M ascorbic acid (pH 5.0).

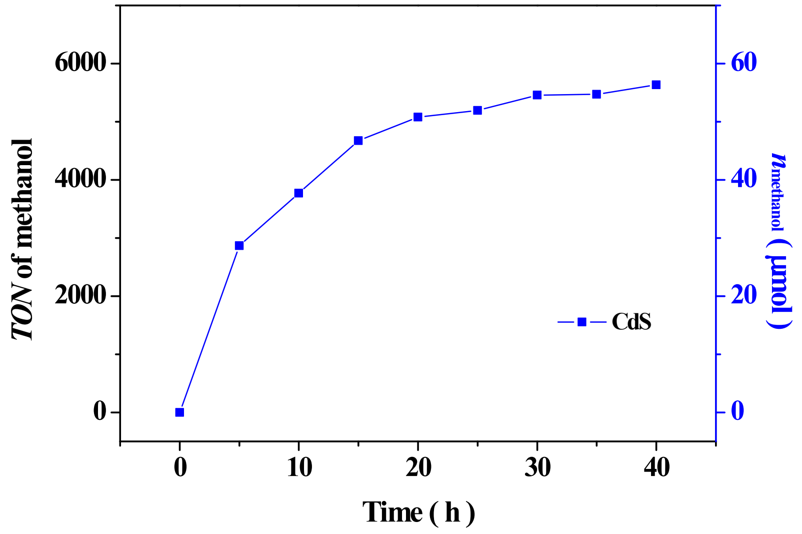

Fig. S13. Methanol evolution kinetics obtained upon continuous visible irradiation (λ = 469 nm) of a pH 5.0 buffer solution containing CO_2 (1 atm), 0.10 mg·mL^{-1} CdS NRs, 0.10 M ascorbic acid, and 0.01 mM Cu-ATSM.

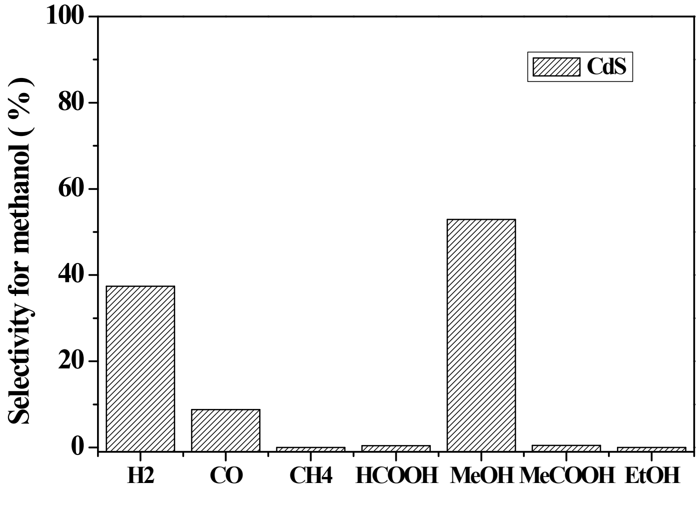

Fig. S14. The selectivity for CO_2 reduction products from the photolysis of the CO_2-saturated $KHCO_3$ (0.10 M) solution (pH 5.0) containing 0.10 mg·mL^{-1} CdS NRs, 0.10 M ascorbic acid and 0.01 mM Cu-ATSM.

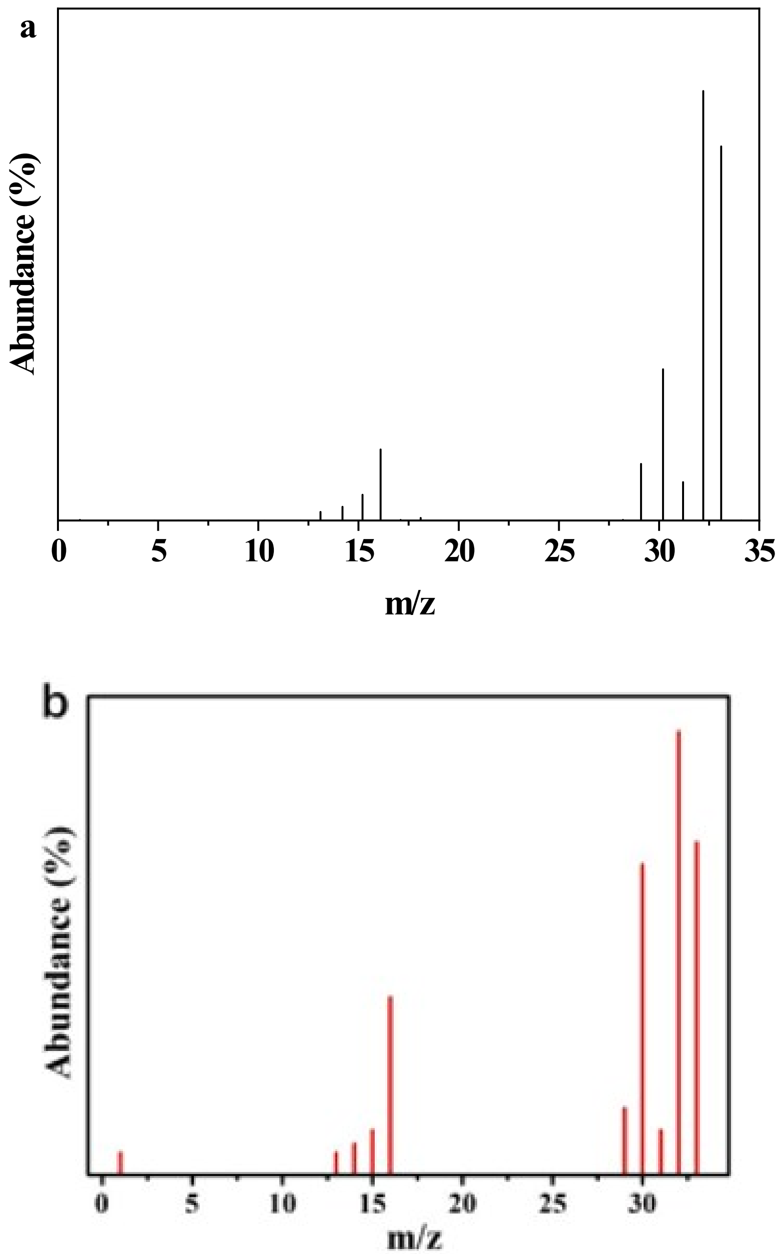

Fig. S15. (a) GC-MS spectrum of $^{13}CO_2$ reduction product mediated by Cu-ATSM. (b) The standard spectrum of $^{13}CH_3OH$.

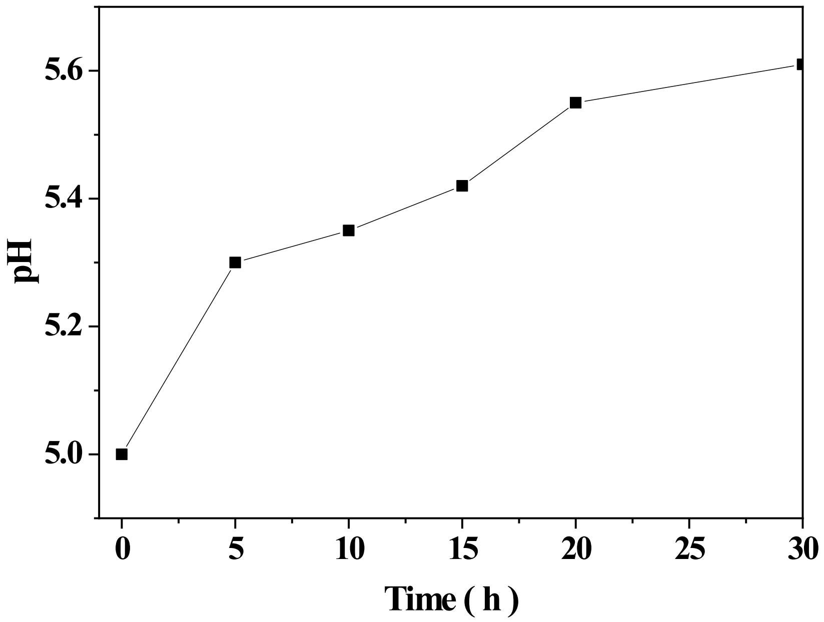

Fig. S16. pH values change of the catalytic system containing CO_2 (1 atm), 0.10 M ascorbic acid, 0.10 mg.mL^{-1} Au-CdS NCs and 0.01 mM Cu-ATSM during photolysis.

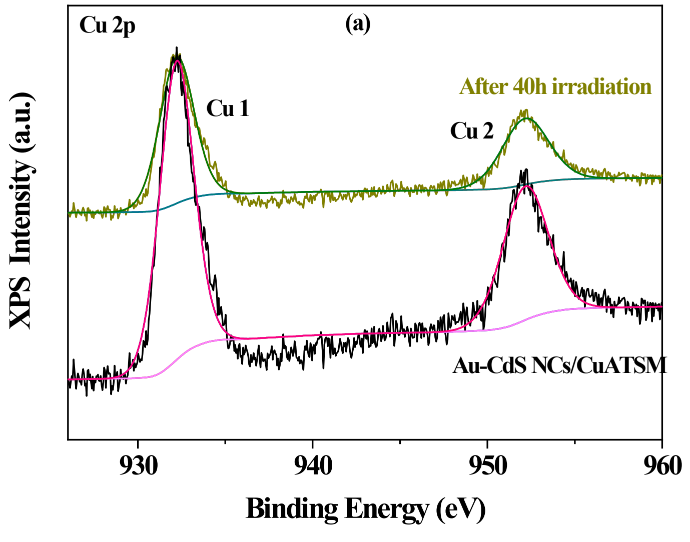

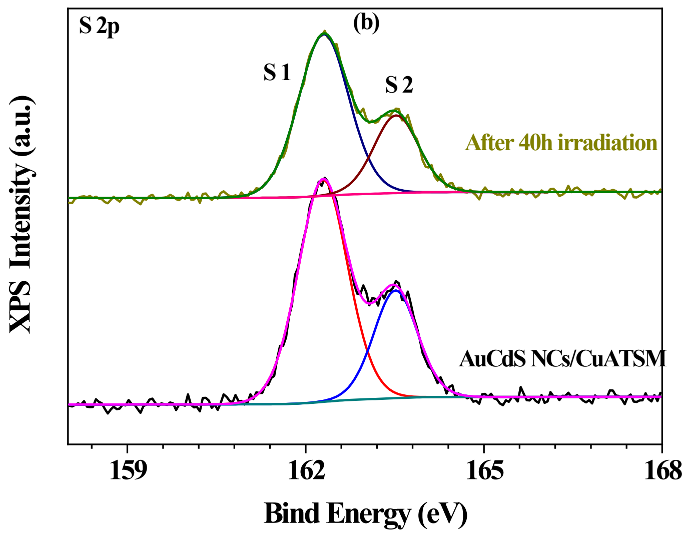
S 2p
(b)
S 1
S 2
After 40h irradiation
AuCdS NCs/CuATSM
XPS Intensity (a.u.)
159
162
165
168
Bind Energy (eV)

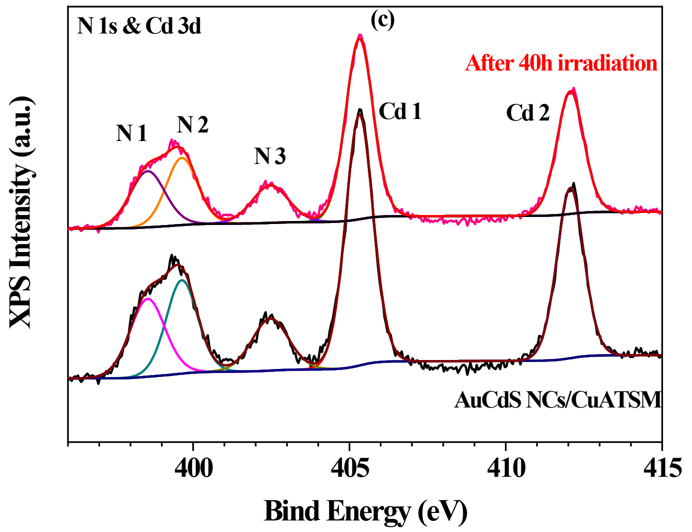
N 1s & Cd 3d
(c)
After 40h irradiation
N 1
N 2
N 3
Cd 1
Cd 2
AuCdS NCs/CuATSM
XPS Intensity (a.u.)
400
405
410
415
Bind Energy (eV)

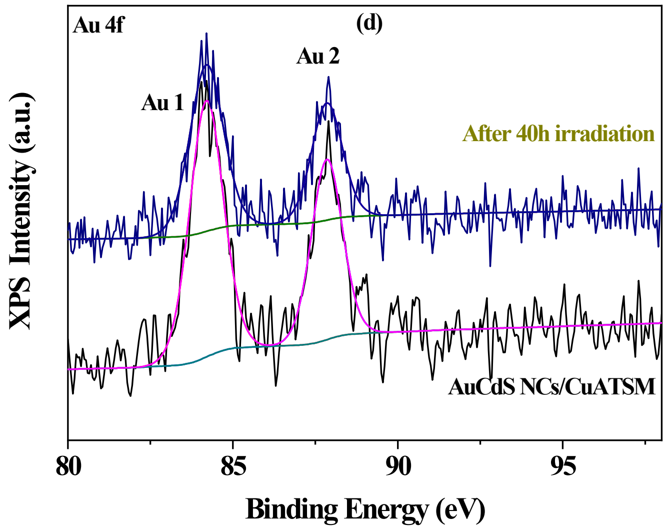

Fig. S17. XPS spectra of the photocatalyst samples. The lower line is for the mixture of Au-CdS NCs and Cu-ATSM. The upper line is the photocatalyst after the CO_2 reduction reaction, which was centrifuged and washed by water after 40 hours of irradiation. (a) High resolution spectra of Cu 2p peaks at 932.18 eV and 952.20 eV. (b) High resolution spectra of S 2p peaks at 162.33 eV and 163.52 eV. (c) High resolution spectra of N 1s and Cd 3d peaks at 398.49 eV, 399.62 eV, 402.47 eV, 405.29 eV and 412.05 eV. (d) High resolution spectra of Au 4f peaks at 84.21 eV and 87.87 eV.

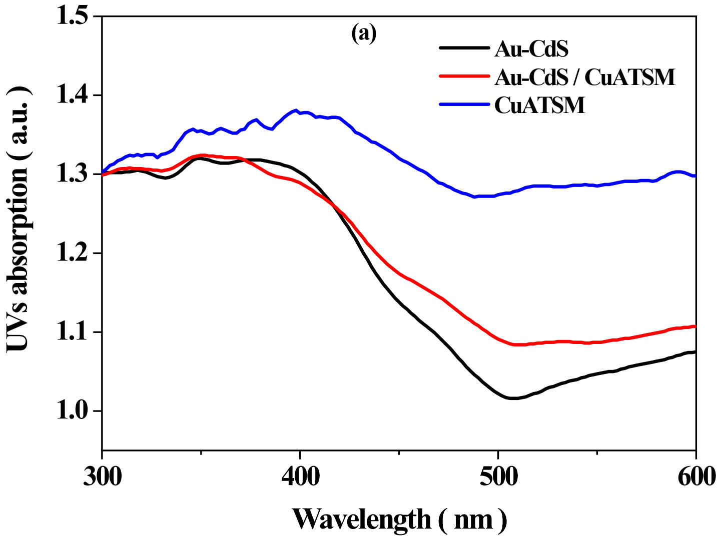

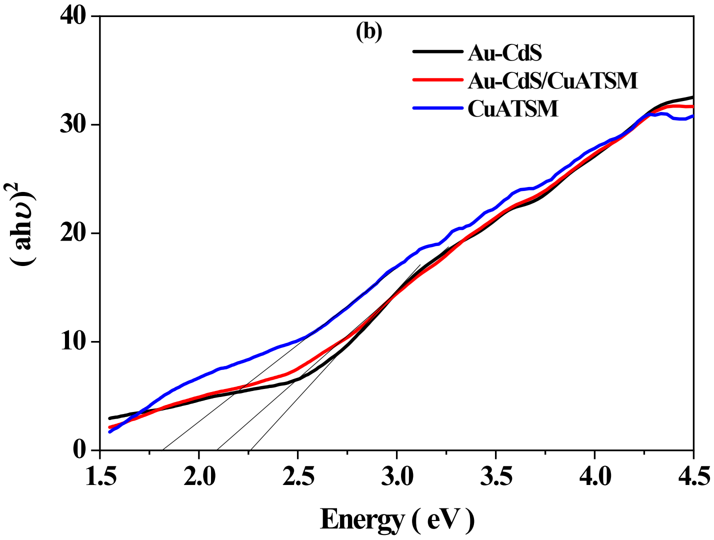

Fig. S18. (a) UV-vis diffuse reflectance spectra of the prepared Au-CdS NCs (black line), Cu-ATSM (blue line) and the mixture of Cu-ATSM and Au-CdS NCs (red line). (b) The estimated band gap spectra obtained from (a).

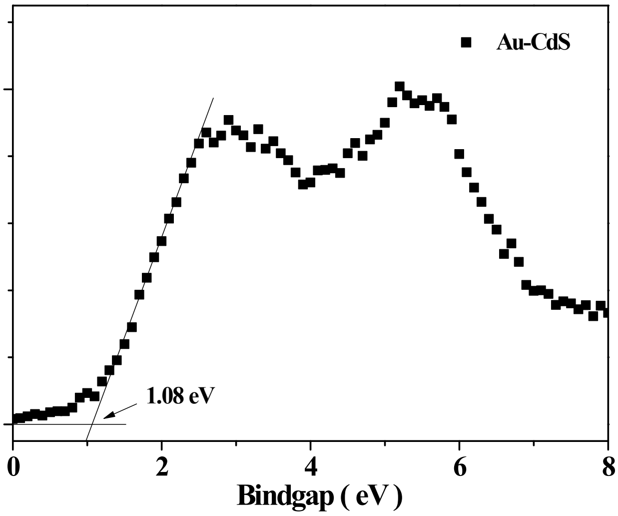

Fig. S19. XPS valence band spectrum of Au-CdS NCs.

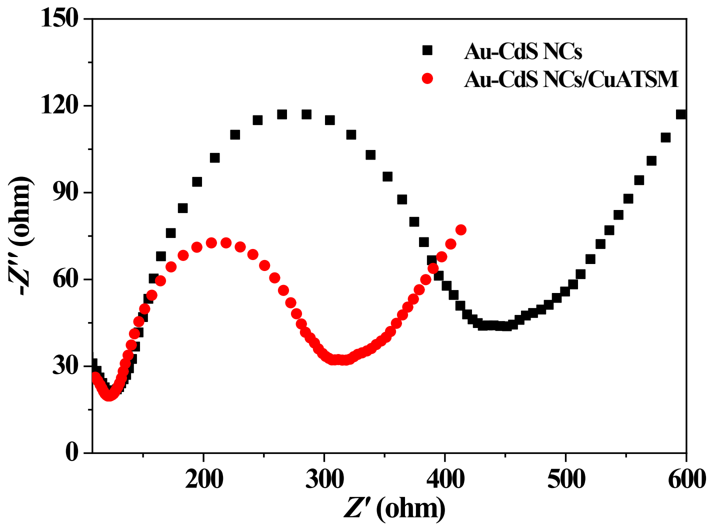

Fig. S20. Electrochemical impedance spectroscopy Nyquist plots of Au-CdS NCs and Au-CdS NCs/Cu-ATSM with FTO electrode (1 cm^2) in 0.010 M $K_3Fe(CN)_6$/ $K_4Fe(CN)_6$ electrolyte in the dark.

Table S1 Crystallographic data for the copper complex, Cu-ATSM

Empirical formula	$C_8H_{15}CuN_6S_2$
Formula weight	322.92
Temperature/K	293(2)
Space group	C-2yc
a/Å	12.3838(17)
b/Å	13.0495(13)
c/Å	8.3122(9)
α/°	90
β/°	90.576(11)
γ/°	90
Volume/Å^3	1343.2(3)
Z	4
ρ_{calc}g/cm^3	1.597
F(000)	664
Radiation	MoKα (λ = 0.71073)
2θ range for data collection/°	3.9610 to 25.1720
Reflections collected	4486
Data/restraints/parameters	1661/14/154
Goodness-of-fit on F^2	0.992
Final R indexes [I>=2σ (I)]	$R_1 = 0.0423$, $wR_2 = 0.0616$
Final R indexes [all data]	$R_1 = 0.0603$, $wR_2 = 0.0676$

Table S2 Selected bond lengths (Å) for the copper complex, Cu-ATSM

Cu(1)–N(1)	1.990(16)	Cu(1)–N(2)	1.925(16)
Cu(1)–S(1)	2.249(6)	Cu(1)-S(2)	2.226(6)